Unprecedented formation of binuclear copper(II) complex with a perylene derived ligand by the oxidative reaction

Jun Hagiwara*[a], Yuichi Shimazaki[b], and Gunzi Saito[c]

[a]*Division of Chemistry, Graduate School of Science, Kyoto University, Kitashirakawa Oiwake-cho, Sakyo-ku, Kyoto 606-8502, Japan*

[b]*College of Science, Ibaraki University, Bunkyo, Mito, 310-8512, Japan*

[b]*Frontier Research Center for Applied Atomic Sciences, Ibaraki University, , Bunkyo, Mito, 310-8512, Japan*

[c]*Research Institute, Meijo University, Shiogamaguchi 1-501 Tempaku, Nagoya 468-8502, Japan*

Received

* Corresponding author. Tel: +81-75-753-4062

E-mail address: hagiwara@kuchem.kyoto-u.ac.jp

Abstract

A new perylene-pendent tridentate ligand, *N*-(3-perylenylmethyl)-*N*,*N*-bis(2-pyridylmethyl)amine (perbpa) **1** and its Cu(II) complex, [Cu(perbpa)Cl$_2$] (**2**) were prepared and structurally characterized by the X-ray diffraction method. In the packing structure of ligand **1**, perylene groups were aggregated to form a π-π stacked layer of dimerized pelylene moieties similar to the packing of pristine perylene. This result suggests both that the π-π interactions among the perylene moieties predominate for the arrangement of perbpa molecules in the crystal and that this ligand is a good candidate for constructing electron conducting path. A complex **2** was prepared from the ligand **1** and a copper(II) chloride dehydrate. **2** had a mononuclear and 5-coordinate distorted square pyramidal structure with a perbpa and two coordinated chloride ions. The chemical oxidation of **2** by iodine resulted in the unprecedented binuclear Cu(II) species, [Cu$_2$(μ-Cl)$_2$(perbpa)$_2$](I$_3$)$_2$, **3**·(I$_3$)$_2$. An X-ray crystal structure analysis of **3**·(I$_3$)$_2$ revealed the binuclear structure bridged by the chloride ions. A temperature dependent magnetic susceptibility measurement of **3** showed a weak ferromagnetic exchange interaction with $S = 1$ ground state, $g = 2.12$ and $J = +1.17$ cm^{-1}, based on $\boldsymbol{H} = -2J\boldsymbol{S_1}\cdot\boldsymbol{S_2}$. The UV-vis absorption and the EPR spectra of **3** showed that the perylene groups are not oxidized. These results indicate a couple of Cu(II) constructed $S = 1$ ground state with intermolecular ferromagnetic interaction. The electrochemical study suggested that the crystallization of **3**·(I$_3$)$_2$ was initiated by the oxidation of the *N*,*N*-bis-(2-pyridylmethyl)amino (bpa) groups of **2** by I$_2$.

Keywords: binuclear copper(II) complex; perylene based ligand; chemical oxidation; magnetic property; electrochemical property.

Introduction

Molecular-based system with a synergetic interaction between magnetic and transport properties has been extensively studied in the past two decades because such a system is fascinating from a theoretical [1, 2] and phenomenological [3] point of view [4]. In order to construct such a system, tetrathiafulvalene (TTF, Scheme 1) derivatives with coordinating groups have been developed [5]. We previously reported that the reaction of TTF-pendent bis(pyridylmethyl)amine (TTFbpa) (Scheme 1) with the Fe(III) ion gave an Fe(II) complex coordinated with oxidized TTF ligand [6]. Even though TTFbpa is a tridentate, flexible, and redox-active ligand, the conducting path of the stacked π-system was not formed due to the mismatch in size between the TTF group and the transition metal coordination centre. In order to resolve this mismatch, replacement of the TTF group by the larger π donor may be required. With these points in mind, we investigated Cu(II) complexes of newly synthesized perylene-pendent bpa ligand (Scheme 1). Perylene has a large π-conjugated electronic system with moderate electron donating ability. The charge transfer complex of perylene and bromine is known as the first molecular-based conductor [7]. A Perylene-based radical ion and group 10 metal ion salts (Ni, Pd, and Pt), (perylene)$_2$[M(mnt)$_2$] (mnt represents maleonitriledithiolate), have been reported as π-d coexisting and cooperating systems[8]. Herein we report the synthesis, X-ray crystal structure determination, and magnetic and spectroscopic characterizations of the mononuclear and binuclear Cu(II) complexes containing a new perylene-pendent-bpa ligand, perbpa (**1**).

2. Experimental

2.1. Materials and methods

Sodium cyanotrihydroborate was purchased from Wako Pure Chemical Industries. 2,2'-Dipicolylamine and tetra-*n*-buthylammonium triiodide (*n*-Bu$_4$NI$_3$) were purchased from Tokyo Chemical Industry. Copper(II) chloride dihydrate, and iodine were purchaced from Nacalai tesque. 3-Perylenecarbaldehyde was prepared according to the literature [9]. All solvents were purified by conventional methods [10]. ^{1}H NMR spectra were recorded on a JEOL JNM-FX400 spectrometer operating at 400 MHz. Melting point was measured on a Yanaco MP-500D micro melting point apparatus and was not corrected. UV‑vis spectra of solid samples using KBr disk method were recorded on a

SHIMADZU UV-3100 spectrophotometer. UV-vis spectra of solutions were recorded on a JASCO V-670 spectrophotometer. The temperature dependence of static susceptibility measurements of the polycrystalline samples was carried out on a superconducting quantum interference device (SQUID) magnetometer of Quantum Design MPMSR2-XL from 2 K to 300 K at 0.1 T. Magnetization data were corrected for sample folder and for diamagnetic contribution calculated from Pascal's constants [11]. Elecron paramagnetic resonance (EPR) spectra of the polycrystalline samples were recorded on a JEOL JES-TE200 X-band (9 GHz) ESR spectrometer equipped with a JEOL ES-CT470 cryostat from 4 K to 300 K. EPR spectrum of dimethylformamide (DMF) frozen solution in 77 K was recorded on a JEOL JES-RE1X X-band spectrometer equipped with a standard low-temperature apparatus. Cyclic voltammetry (CV) and differential pulse voltammetry (DPV) measurements were carried out on the DMF solution of 0.1 M n-Bu$_4$NClO$_4$ $vs.$ Ag/AgCl by means of an ALS/chi electrochemical analyzer model 650A at room temperature under nitrogen atmosphere. Voltammograms were recorded with a platinum disk and a platinum wire for working and counter electrodes, respectively. Sweeping velocity was 10 mV s^{-1}.

*2.2. Synthesis of ligand, N-(3-perylenylmethyl)-N,N-bis(2-pyridylmethyl)amine (perbpa) (**1**).*

A 1,2-dichloroethane solution (50 ml) of 3-perylenecarbaldehyde (1.4 g, 5.0 mmol) and acetic acid (1.0 ml) were added to an ethanol solution (50 ml) of 2,2'-dipicolylamine (1.0 g, 5.0 mmol). To the mixture was added sodium cyanotrihydroborate (90%, 0.36 g, 5.2 mmol). After the reaction mixture was refluxed for 2 hours under argon atmosphere, it was concentrated to dryness under a reduced pressure and acidified with 1 M HCl aqueous solution (50 ml). The acidic solution was neutralized with saturated sodium hydrogen carbonate, and extracted with chloroform (2 × 50 ml). The combined organic layer was washed with brine (100 ml), dried over anhydrous sodium sulfate, and evaporated to give red solid, which was purified by silica gel column chromatography (at first chloroform and successively chloroform/methanol 20/1 (v/v)). The crude product (yellow powder) was recrystallized from benzene to give yellow platelets (1.1 g, 48%). ^{1}H NMR (CDCl$_3$, δ / ppm vs. TMS) 8.53 (m, 2H, py-H), 8.15 (m, 4H, py-H), 7.97 (d, J = 8.4 Hz, 1H, per-H), 7.63 (m, 5H, per-H), 7.46 (m, 5H, per-H), 7.13 (m, 2H, py-H), 4.08 (s, 2H, per-CH$_2$), 3.90 (s, 4H, py-CH$_2$). mp. 184-185 °C. Elemental analysis (%) calcd. for C$_{33}$H$_{25}$N$_3$, C 85.50 H 5.44 N 9.06; found,

C 85.74 H 5.38 N 8.97.

2.3 Syntheses of Cu(II) complexes

2.3.1. [Cu(perbpa)Cl$_2$]·0.5H$_2$O (2·0.5H$_2$O).

To a methanol solution (10 mL) of CuCl$_2$·2H$_2$O (0.094 g, 0.55 mmol) was added **1** (0.24 g, 0.52 mmol) in dichloromethane (10 mL). The reaction mixture was filtrated and the filtrate was slowly evaporated to yield green platelets (0.24 g, 78%). mp. 219 °C dec. Elemental analysis (%) calcd. for C$_{33}$H$_{26}$N$_3$Cl$_2$CuO$_{0.5}$, C 65.29 H 4.32 N 6.92 Cl 11.68; found, C 65.28 H 4.51 N 6.90 Cl 11.58.

2.3.2. [Cu$_2$(μ-Cl)$_2$(perbpa)$_2$]I$_{5.6}$ (3·I$_{5.6}$)

A methanol solution (10 mL) of CuCl$_2$·2H$_2$O (0.016 g, 0.094 mmol) was mixed with a dichloromethane solution (10 mL) of **1** (0.049 g, 0.11 mmol). Iodine (0.050 g) was added to the green reaction mixture and heated. After iodine was completely dissolved, the hot dark red solution was filtrated and the filtrate was left to stand for 3 days at room temperature to give deep red prisms (0.046 g, 47%). mp. 202 °C dec. Elemental analysis (%) calcd. for C$_{66}$H$_{50}$N$_6$Cl$_2$Cu$_2$I$_{5.6}$, C 43.18 H 2.75 N 4.58; found, C 43.13 H 2.52 N 4.34. Owing to the volatile nature of iodine, the composition estimated from elemental analysis was different from that determined by X-ray diffraction analysis (*vide infra*).

2.4 Crystal structure determinations

The X-ray experiment for **1** was carried out for the well-shaped single crystal on a MAC Science DIP-2020K imaging plate diffractometer with graphite monochromated Mo Kα radiation (λ = 0.71073 Å) at 293 K. The structure was solved by direct method. The refinement of structure was performed by full matrix least square method on F^2. The parameters were refined adopting anisotropic temperature factors for non-hydrogen atoms. The positions of hydrogen atoms were determined by calculation assuming sp^2 or sp^3 conformation and C-H bond length of 0.95 Å. The parameters were refined adopting isotropic temperature factors for hydrogen atoms.

The X-ray experiments for **2** and **3** were carried out for the well-shaped single crystals on a Rigaku RAXIS imaging plate area detector with graphite monochromated

Mo Kα radiation (λ = 0.71073 Å) at 130 K. In order to determine the cell constants and orientation matrix, three oscillation photographs were taken for each frame with the oscillation angle of 3° and the exposure time of 3 min. Reflection data were corrected for both Lorentz and polarization effects. The structures were solved by the heavy-atom method and refined anisotropically for non-hydrogen atoms by full-matrix least-squares calculations. Atomic scattering factors and anomalous dispersion terms were taken from the literature [12]. Hydrogen atoms except those of the water molecules were located at the calculated positions and were assigned a fixed displacement and constrained to ideal geometry with N–H = 0.90 Å and C–H = 0.95 Å. The thermal parameters of calculated hydrogen atoms were related to those of their parent atoms by $U(H) = 1.2U_{eq}(C, N)$. All the calculations were performed by using the Rigaku CrystalStructure ver. 3.5.1 program package. Summaries of the fundamental crystal data and experimental parameters for structure determination are given in Table 1.

3. Results and discussion

3.1. Preparation of perylene-linked ligand and its copper(II) complexes

The Cu(II) complex of $[Cu(perbpa)Cl_2]$ (**2**) was synthesized by a reaction of ligand **1** with $CuCl_2 \cdot 2H_2O$ at room temperature. The single crystals for X-ray analysis contain methanol (MeOH) for crystallization, and so the composition of the Cu(II) complex estimated from X-ray analysis is **2**·MeOH. The methanol easily escapes from crystals under ambient pressure. After removal of methanol by drying under reduced pressure of 0.1 Torr at room temperature for 2 h, water was incorporated into the sample; and so the composition of the complex determined by an elemental analysis was therefore **2**·0.5H_2O. In order to obtain conducting material, chemical oxidation by iodine was carried out for the mixture of ligand **1** and $CuCl_2 \cdot 2H_2O$. Dark red prisms of **3**·$(I_3)_2$ were obtained by the reaction with I_2 in the $MeOH/CH_2Cl_2$. I_3^- anion in **3** was partially sublimed to form I^- anion even at ambient conditions. Elemental analysis reproducibly determined the composition to be $[Cu_2Cl_2(perbpa)_2]I_{5.6}$, which is assigned to $[Cu^{2+}_2Cl^-_2(perbpa^0)_2](I_3)^-_{1.8}(I)^-_{0.2}$ since the optical and magnetic measurements confirmed that the the charges on the Cu, perbpa, and Cl⁻ species remained the same before and after the sublimation of I_2. All of the synthetic schemes are summarized in Scheme 2.

3.2. Crystal structures

1 crystallizes in the orthorhombic system (*Pbnb*). The molecular structure of **1** is shown in the Supplementary material. Fig. 1a shows the *b*-axis projection for the packing structure of **1**. Bond lengths of the perylene group are similar to those of the neutral form [13]. This results suggests that perylene moiety in **1** also is the neutral form. The interesting point is the formation of a two-dimensional segregated layer of the perylene groups in the *ab*-plane. This layer is composed of orthogonally aligned dimerized perylene groups (Fig. 1b). Such a packing structure is similar to that observed for neutral perylene crystal (*α*-form) [13]. The interplanar distance within a dimer is 3.45 Å, which is as long as that of the neutral perylene (3.45 Å) [13]. These facts indicate that the π-π interactions within the perylene layers predominate for the arrangement of perbpa molecules in the crystal and that ligand **1** has high potential to form a carrier path required for electric conductors. The two-dimensional perylene layers, with a the width of ca. 9 Å for each, are separated by a thick layer (ca. 9 Å) composed of bpa groups along the *c*-axis (Fig. 1a).

2·MeOH crystallizes in the monoclinic system (*P2₁/n*). The molecular structure is shown in Fig. 2a. Selected bond distances and angles are summarized in Table 2. The X-ray crystal structure revealed that **2**·MeOH is a mononuclear penta-coordinate structure that incrudes two chloride ions, two pyridine nitrogens, and an amine nitrogen with Cu-N bond lengths of Cu-N(1) 2.007 (4) Å, Cu-N(2) 2.046 (4) Å, and Cu-N(3) 2.012 (4) Å (Fig. 2a, Table 2). The axial Cu-Cl(2) distance (2.592 (1) Å) is longer than the other Cu-Cl(1) distance (2.247 (1) Å), this difference originated from the Jahn-Teller distortion typical for a Cu(II) complex of d^9 electronic configuration. The coordination geometry in **2**·MeOH can therefore be described as a distorted square pyramid. The bond lengths of the perylene group are similar to those of non-functionized perylene [13]. An interesting point in the molecular structure for **2**·MeOH is that the perylene moiety faces to one of the pyridine moiety, which coordinates the Cu(II) centre (Fig. 2a). This suggests a π-π stacking between the pyridine and perylene moieties. The distance between the pyridine moiety and the perylene moiety was estimated to be ca 3.67 Å, although these moieties were not parallel. These facts suggest that a weak π-π interaction exists between pyridine and perylene moieties.

In the packing structure, a couple of perylene moieties of **2** form a dimer (Fig.

7

2b) with the aid of the π-π interaction between the perylene groups with a interplanar distance of 3.42 Å, which is a slightly shorter than the interplanar distance for nonfunctionalized perylene. Therefore, one perylene dimer is sandwiched by two pyridine rings to form a unit of pyridine-perylene-pyridine-perilene, encircled in Fig. 2b, and the units are arranged along the *b*-axis. However the conduction path for π-electron is deteriorated, by the inclusion of MeOH as depicted in Fig. 2b.

$3 \cdot (I_3)_2$ crystallizes in the triclinic ($P\bar{1}$) system. This complex consists of a binuclear $[(perbpa)Cu(\mu\text{-}Cl)_2Cu(perbpa)]^{2+}$ ion and two I_3^- as counteranions. Bond lengths and angles of the coordination sphere are summarized in Table 2. Figure 3a depicts the molecular structure of **3**. The bridging Cu_2Cl_2 unit is constrained to be planar, and the crystallographic inversion centre is allocated at the middle of the molecule. Each Cu ion in $3 \cdot (I_3)_2$ is coordinated to three nitrogen atoms in the perbpa ligand and two chloride ions in a slightly distorted square-pyramidal geometry. Similar to the structure of **2**·MeOH, one chloride ion is in the basal plane (Cu1-Cl1 = 2.257(1) Å) and another chloride ion is located on the apical position (Cu1-Cl1'= 2.643(1) Å). Two square pyramids share a base-to-apex edge so that the Cl atom situated at the vertex of one base becomes the apical vertex of the other square pyramid, and the opposite happens for the other Cl-bridging ligand. Such a coordination structure was categorized as 'parallel-type' in literature [14]. The bond angle of Cu1-Cl1-Cu1' is 84.29(4)°. Bond lengths of the perylene group in $3 \cdot (I_3)_2$ are similar to those of the neutral perylene molecule and those in **2**·MeOH. In the molecular structure, in contrast to that of **2**·MeOH, the perylene group faces opposite side of the coordination centre and not stacks with pyridine groups coordinating to Cu(II) (Fig. 3a). In the packing structure, perylene groups form dimers, which are isolated with an intradimer perylene plane distance of 3.47 Å, slightly longer than that for nonfunctionalized perylene (Fig. 3b). This indicates that the conduction path neither exists in $3 \cdot (I_3)_2$.

3.3 Optical spectra

The UV-vis absorption spectrum of **2**·0.5H$_2$O in DMF solution showed four peaks (375, 398, 422, and 448 nm) (Fig. 4). These peaks are assignable to a perylene π-π* transition band with a vibronic structure (368, 387, 409, and 435 nm in cyclohexane [15]). The spectrum of $3 \cdot I_{5.6}$ was a superposition of the absorption of **2** and

that of n-Bu$_4$NI$_3$ (365 nm). The absorption spectrum of the solid state, using the KBr method, corresponded to the absorption spectrum in solution (Fig. 5). A small absorption band at $12–13 \times 10^3$ cm$^{-1,}$ seen for 3·I$_{5.6}$ in the KBr method, is assignable to the d-d band of the Cu(II) centre. These results suggest that the perylene group in **3** is not cationic but in the neutral electronic state.

3.4 Magnetic properties of copper complexes.

Temperature dependences of the χT products for **2**·0.5H$_2$O and **3**·I$_{5.6}$ are shown in Fig. 6. **2**·0.5H$_2$O shows Curie−Weiss (eq. 1) behaviour typical for a square-pyramidal mononuclear Cu(II) complex ($S = 1/2$, $g = 2.13$, $\Theta = -0.265$ K):

$$\chi = \frac{Ng^2\mu_B^2 S(S+1)}{3k(T-\Theta)} \quad . \tag{1}$$

On the other hand, the χT product for **3**·I$_{5.6}$ behaves differently from that of **2**·0.5H$_2$O. The χT product at 300 K is 0.901 emu K mol^{-1} for 3·I$_{5.6}$, which is a reasonable value for noninteracting two $S = 1/2$ spins ($\chi T = 0.902$ for $g = 2.06$). At low temperatures, the χT product slightly increases due to the intramolecular ferromagnetic coupling of chloride bridged Cu(II) centres. The simple Bleany−Bowers equation [16] is unacceptable for these compounds because singlet-triplet energy gaps estimated based on the basis of such an equation are comparable to Zeeman splitting ($|E_{S-T}| = 2|J| \sim g\mu_B H$). Friedberg's magnetization expression [17] is applied for fittings of the data. Friedberg's expression is given by eqs. 2 and 3,

$$M = \frac{2Ng\mu_B \sinh(g\mu_B H/kT)}{\exp(-2J/kT) + 2\cosh(g\mu_B H/kT) + 1} \tag{2}$$

$$\chi - N\alpha = M/H \tag{3}$$

for isotropic exchange Hamiltonian of eq. 4

$$\hat{H} = -2J\hat{S}_1 \cdot \hat{S}_2 \tag{4}$$

, where $N\alpha$ is a temperature-independent paramagnetism. The susceptibility data are fitted to the values of $g = 2.12$, $J = +1.17$ cm^{-1}, and $N\alpha = 1.55 \times 10^{-4}$ emu mol^{-1} for **3**·I$_{5.6}$. The excellent fit and small J value together with such 'parallel-type' geometry indicate

that the magnetic interaction between the copper centres takes place mainly through a π^* type of interaction between Cu $d_{x^2-y^2}$ and the apical p_{Cl} orbitals, which is in good agreement with previous theoretical and experimental works [14].

An X-band EPR spectrum of a polycrystalline sample of $\mathbf{3}\cdot I_{5.6}$ at 4 K provided detailed information about the spin state. $\mathbf{3}\cdot I_{5.6}$ showed g-tensor anisotropy with $g_{//} = 2.122$ and $g\perp = 2.054$. Moreover, a half-field resonance of $g = 4.235$ ($\Delta Ms = \pm 2$) was observed in the spectrum. The half-field resonance decreased as temperature increased even though the signal remained at 300 K. This result clearly indicates the triplet ($S = 1$) ground state of the Cu(II) binuclear system. The EPR spectrum of a DMF frozen solution of $\mathbf{3}\cdot I_{5.6}$ at 77 K is typical for the spectrum of axially distorted Cu(II) complexes ($g_{//} = 2.224$, $g\perp = 2.041$, and $a_{//} = 17.6$ mT). In a previous work of Fe(II) TTFbpa complex, sharp EPR signals with hyperfine splitting at around $g = 2.00$ originating from the radical state of the TTF group were only detected in an acetonitrile (MeCN) solution but not in a powder sample because of the strong anti-ferromagnetic coupling between the TTF cation radical groups in a solid state [6]. In the case of $\mathbf{3}$, such a sharp EPR signal around $g = 2.00$ was not detected in either a polycrystalline state or in a DMF frozen solution. These magnetic properties for $\mathbf{3}\cdot I_{5.6}$ are consistent with the crystal structure and absorption spectrum.

3.5 Electrochemical studies

From the studies described above, $\mathbf{3}\cdot I_{5.6}$ has a ferromagnetically coupled ground state with two electron spins on each Cu(II) binuclear ion, while the perylene moiety is not in the cation radical state. These results indicate that the chemical oxidation by I_2 did not yield ligand-centred oxidized species but yielded species with neutral ligands. The formation of $\mathbf{3}\cdot I_{5.6}$ proceeded through the formation of I_3^- anion, which was a reduced product of I_2, indicating the redox process is the key step toward compound $\mathbf{3}\cdot I_{5.6}$.

To examine the formation processes, electrochemical properties of ligand $\mathbf{1}$ and the Cu(II) complex $\mathbf{2}\cdot 0.5H_2O$ were investigated. A cyclic voltammogram of $\mathbf{1}$ showed irreversible oxidation peaks at +0.86 V and +0.98 V vs. Ag/AgCl (Fig. 7). Since TTF-pendent ligand TTFbpa exhibited three anodic peaks at +0.232, +0.564, and +0.856 V vs. Ag/AgCl by DPV measurement and the former two peaks correspond to

those of pristine TTF (+0.248 and 0.612 V), the peak at +0.856 V is assignable to that of the bpa moiety in TTFbpa [6]. Even though the measurement condition was different (solvent used in the measurement for TTFbpa was MeCN), the oxidation peak at +0.86 V observed in **1** may be ascribed to that of the bpa moiety in perbpa. The oxidation peak at +0.98 V corresponds to the perylene moiety of **1**. A cyclic voltammogram of **2**·0.5H$_2$O, on the other hand, showed an irreversible oxidation peak at +0.96 V (Fig. 7). The peak at +0.86 V in the voltammogram of **1** is absent in the voltammogram of **2**·0.5H$_2$O because the coordination of the amino group in the bpa moiety to the Cu(II) ion lowered the electron density on the anino-N atom in HOMO, and hence the oxidation potential of the bpa group increased. Oxidation potentials of **1**, **2**·0.5H$_2$O, and perylene in DMF were precisely determined by DPV measurements (Table 3). Scheme 3 shows a plausible mechanism of formation of **3**·(I$_3$)$_2$ based on electrochemical studies. The Cu(II) complex is labile in general, so in the solution of **2**·0.5H$_2$O, a small quantity of perbpa may be released, or Cl$^-$ may be released to generate dinuclear species of **3**. When I$_2$ is added to such a solution, although perbpa coordinating to the Cu(II) ion is inert to oxidation, bpa would be quickly oxidized in the released perbpa. This redox process generates unidentified decomposed species and an I$_3^-$ ion which forms [(perbpa)^{0}Cu^{II}(μ-Cl$_2$)Cu^{II}(perbpa)^0](I$_3$)$_2$.

4. Conclusion

We prepared and characterized a new tridentate ligand, perbpa **1**, containing three nitrogen atoms for coordination and one perylene group for the π-electron reservoir and studied electronic and structural properties of its Cu(II) complexes. The refined crystal structure indicated that ligand **1** has a high potential to form the conduction path required for the electric conductors. The crystal structure of the mononuclear Cu(II) complex **2**·MeOH revealed a distorted square-pyramidal coordination geometry around Cu(II). The reaction of CuCl$_2$·2H$_2$O perbpa and iodine yielded an unprecedented dichloro-bridged binuclear Cu(II) complex **3**·(I$_3$)$_2$ with a neutral perylene-pendent ligand. This binuclear Cu(II) complex exhibited weakly ferromagnetic coupling with two S = 1/2 Cu(II) centres. The formation of an I$_3^-$ anion is due to the oxidation of the bpa group.

5. Supplementary material

Crystallographic data (excluding structure factors) for **1**, **2**·MeOH, and **3**·(I$_3$)$_2$ have been deposited with the Cambridge Crystallographic Data Centre (CCDC) as supplementary publication numbers CCDC-763642 for **1**, 763643 for **2**·MeOH, and 76344 for **3**·(I$_3$)$_2$. Copies of the data can be obtained free of charge on application to CCDC, 12 Union Road, Cambridge CB2 1EZ, UK (fax: (+44)1223-336-003; e-mail: deposit@ccdc.cam.ac.uk). Supplementary data (elemental analysis simulation for **3**, molecular structure of **1**, bond lengths of perylene groups and distances between perylene planes for **1**, **2**·MeOH, and **3**·(I$_3$)$_2$, EPR spectra of **3**·I$_{5.6}$, and DPV voltammograms for 1, **2**·0.5H$_2$O, and perylene can be found in the online.

References

[1] (a) J. Kondo, Prog. Theor. Phys. 32 (1964) 372. (b) R. Ramirez, L. M. Falicov, Phys. Rev. B 3 (1971) 2425.

[2](a) M. A. Ruderman, C. Kittel, Phys. Rev. 96 (1954) 99. (b) T. Kasuya, Prog. Theor. Phys. 16 (1956) 45; (c) K. Yoshida, Phys. Rev. 106 (1957) 893.

[3] (a) G. Binasch, P. Grünberg, F. Saurenbach, W. Zinn, Phys. Rev. B 39 (1989) 4828. (b) M. N. Baibich, J. M. Broto, A. Fert, F. Nguyen Van Dau, F. Petroff, P. Eitenne, G. Creuzet, A. Friedrich, J. Chazelas, Phys. Rev. Lett. 61 (1988) 2472.

[4] (a) E. Coronado, P. Day, Chem. Rev. 104 (2004) 5419. (b)T.Enoki, A. Miyazaki, Chem. Rev. 104 (2004)5449. (c) T. Inabe, Chem. Rev. 104 (2004) 5503.

[5] D. Lorcy, N. Bellec, M. Formigué, N. Avarvari, Coord. Chem. Rev. 253 (2009) 1398 and references herein.

[6] J. Hagiwara, G. Saito, in Multifunctional Conducting Molecular Materials, eds. G.Saito, F. Wudl, R. C. Haddon, K. Tanigaki, T. Enoki, H. E. Katz, M. Maesato, RSC Publishing, Cambridge, UK. (2007) pp. 169.

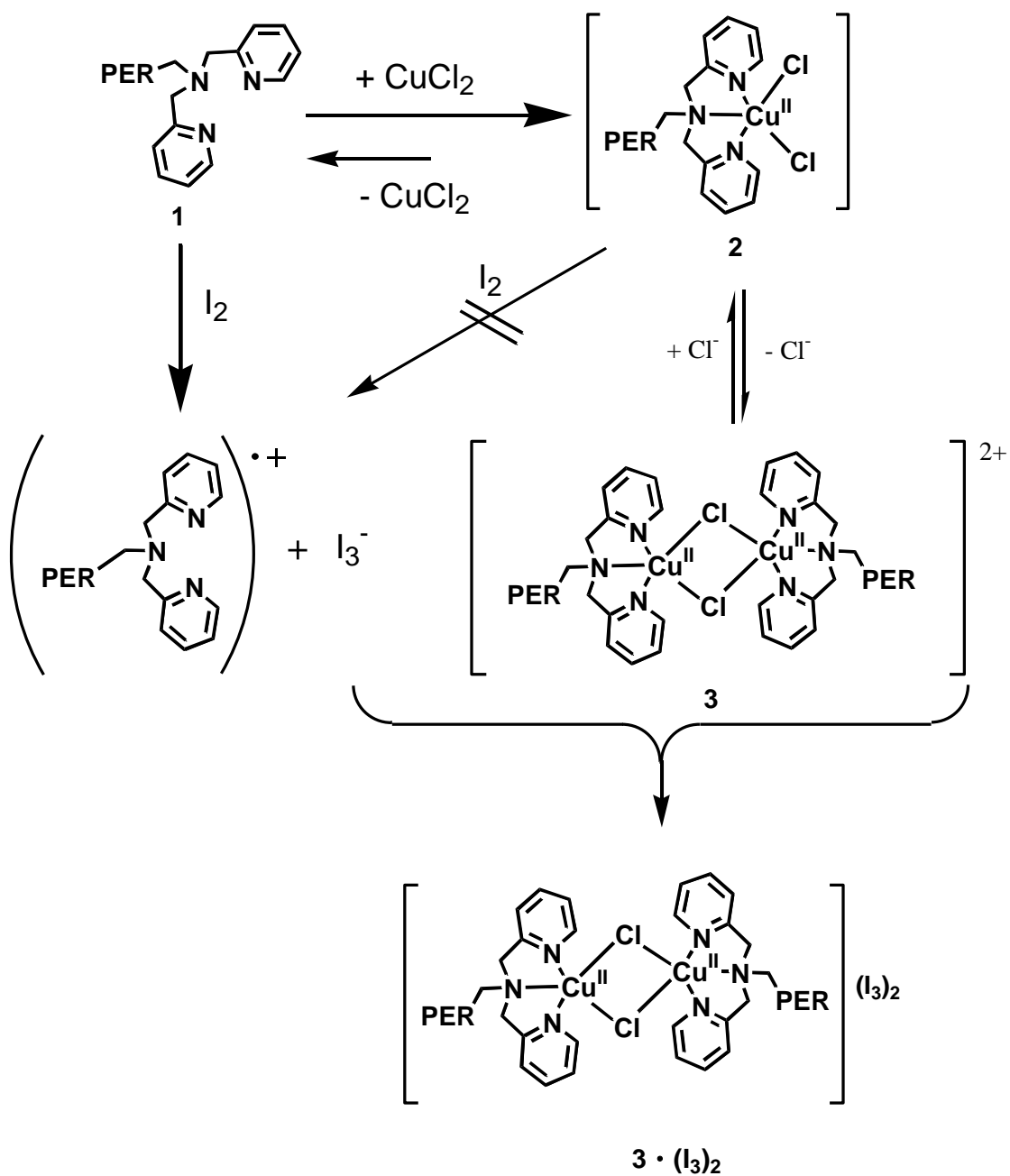[7] H.Akamatu, H.Inokuchi, Y. Matsunaga, Nature 173 (1954) 168.

[8] (a) V. Gama, M. Almeida, R. T. Henriques, I. C. Santos, Â. Domingos, S. Ravy, J. P. Pouget, J. Phys. Chem. 95 (1991) 4263. (b) V. Gama, R. T. Henriques, M. Almeida, L. Alcácer, ibid, 98 (1994) 997.

[9] U. Asseline, E. Cheng, Tetrahedron Lett. 42 (2001) 9005.

[10] D. D. Perrin, W. L. F. Armarego, Purification of Laboratory Chemicals 2nd Ed., Pergamon Press, 1980.

[11] C. J. O'Connor, Prog. Inorg. Chem. 29 (1982) 203.

[12] (a) D. T. Cromer, J. T. Waber, International Tables for X-ray Crystallography, The Kynoch Press, Birmingham Vol. IV (1974). (b) J. A. Ibers, W. C. Hamilton, Acta Crystallogr. 17 (1964) 781. (c) D. C. Creagh, J. H. Hubbell, International Tables for Crystallography, Kluwer Academic Publishers, Boston, Vol. C (1992)

[13] A. Camerman, J. Trotter, Proc. R. Soc. Lond. A279 (1964) 129.

[14] M. Rodríguez, A. Liobet, M. Corbella, Polyhedron 19 (2000) 2483.

[15] H. Du, R. A. Fuh, J. Li, A. Corkan, J. S. Lindsey, Photochem. Photobiol. 68, (1998) 141

[16] B. Bleaney, K. D. Bowers, Proc. R. Soc. Lond. A214 (1952) 451.

[17] B. E. Meyers, L. Berger, S. A. Friedberg, J. Appl. Phys. 40 (1969) 1149.
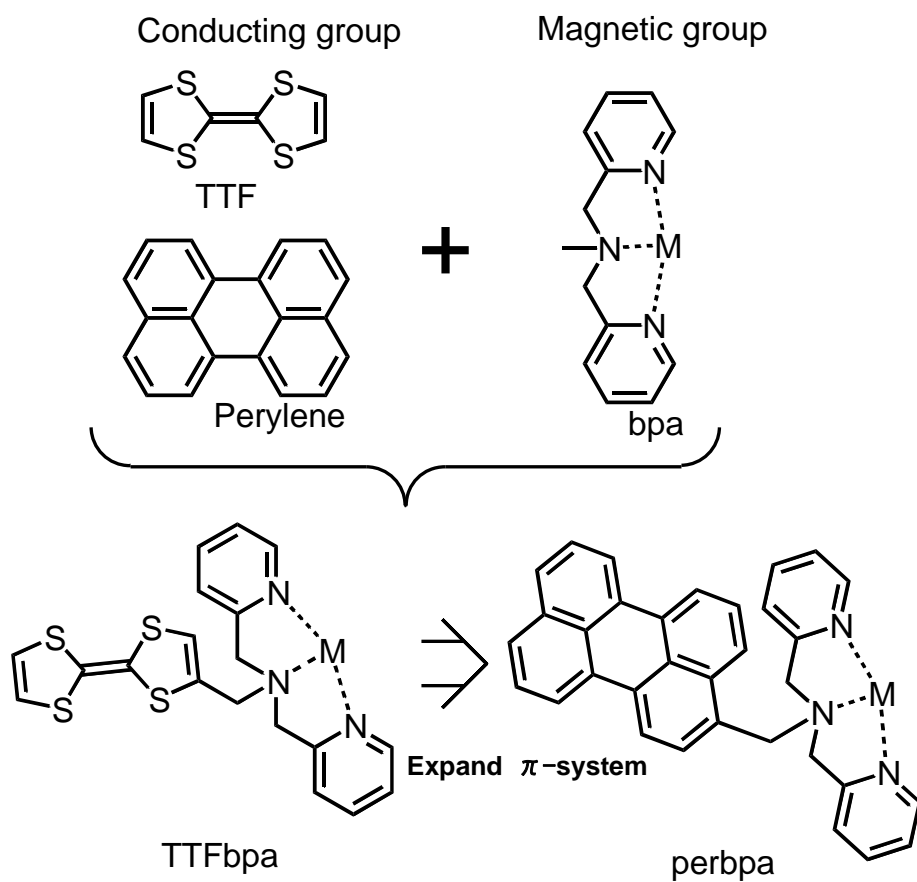
Scheme 1. Molecular design of metal-perbpa complex.

=PER-CHO

NaBH$_3$CN
CH$_3$CO$_2$H
C$_2$H$_5$OH,CH$_2$ClCH$_2$Cl
48%

perbpa **1**

1

CuCl$_2$·2H$_2$O

MeOH, CH$_2$Cl$_2$
78%

[Cu(perbpa)Cl$_2$]·MeOH
2·MeOH

1

CuCl$_2$·2H$_2$O

I$_2$
CH$_3$OH, CH$_2$Cl$_2$
47%

[Cu$_2$(μ–Cl)$_2$(perbpa)$_2$](I$_3$)$_2$
3·(I$_3$)$_2$
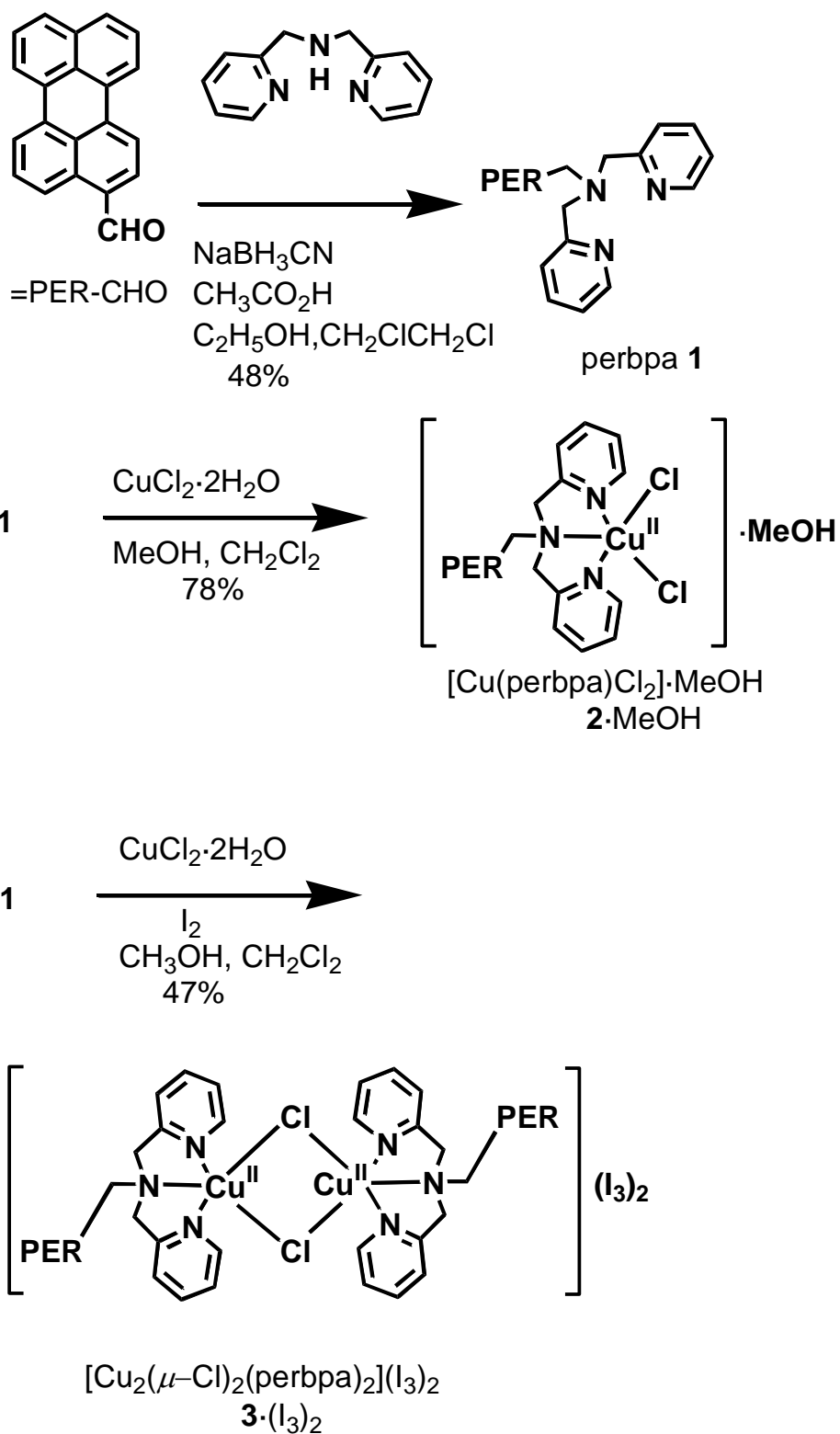
Scheme 2. Synthetic routes for compounds **1**, **2**, and **3**.

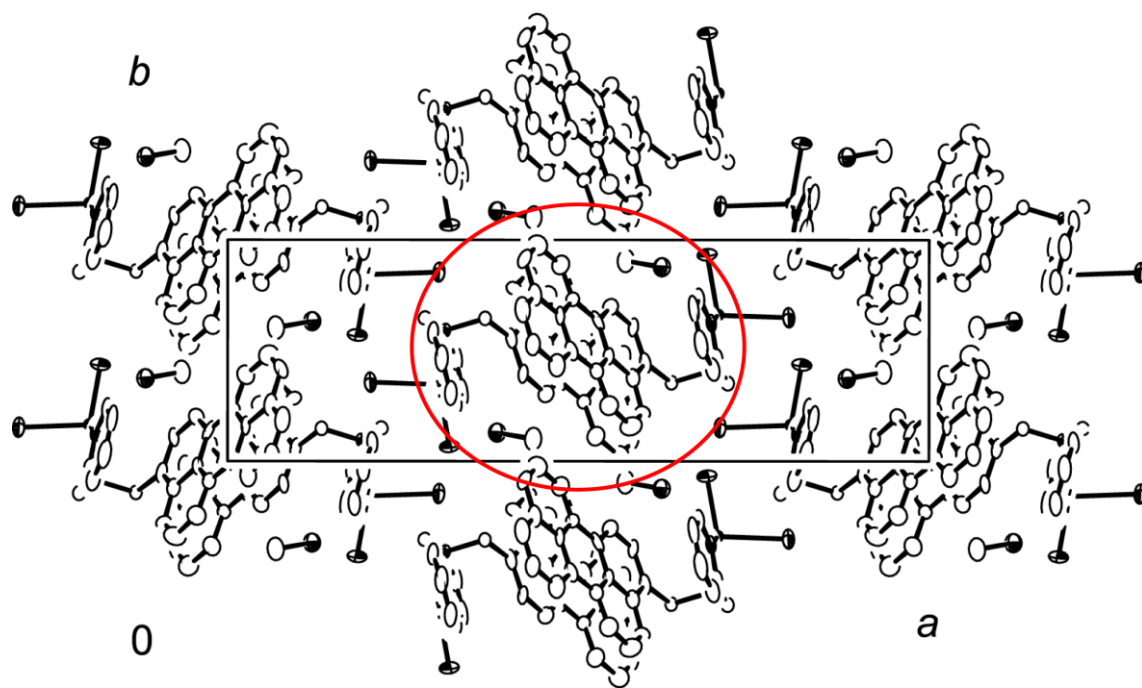Scheme 3. Mechanism of formation of $\mathbf{3}\cdot(I_3)_2$ proposed in this paper.

(a)

(b)
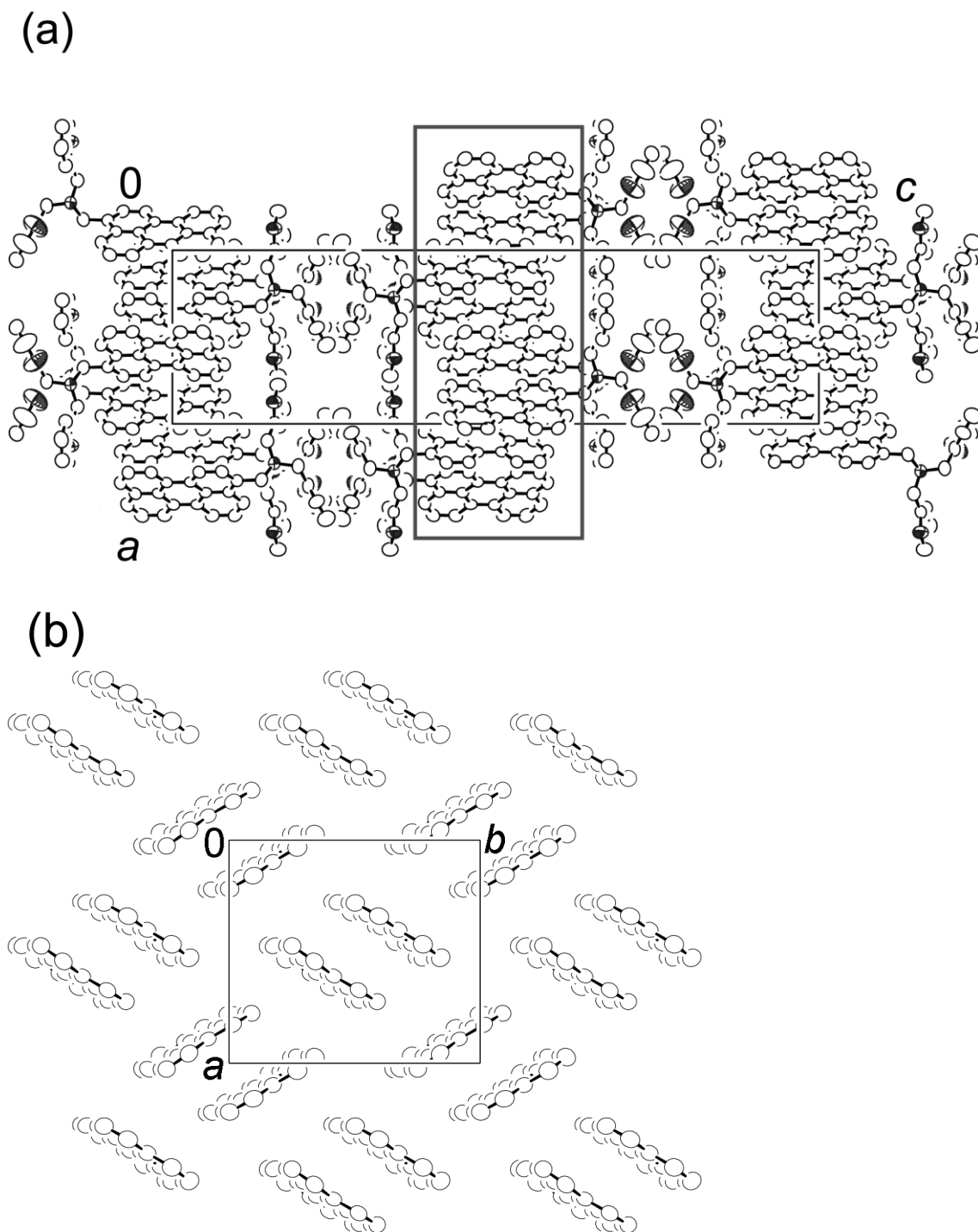
Figure 1. (a) Packing view (b-axis projection) of **1**. A gray square indicates an aggregation of perylene groups. (b) Aggregation mode of perylene moieties of **1** (*c*-axis projection).

(a)
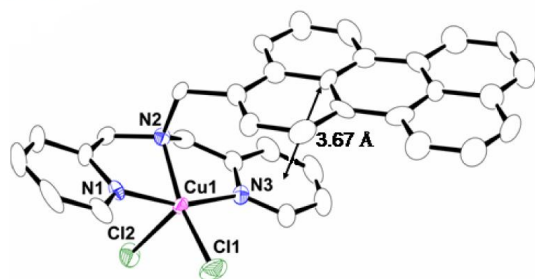
(b)

Figure 2. (a) Molecular structure of **2** in **2**·MeOH with thermal ellipsoids at 50% probability. (b) Packing view (*c*-axis prejection) of. **2**·MeOH. A red ellipsoid represents an aggrregation of pyridine-perylene-perylene-pyridine moieties (see text). Hydrogen atoms are omitted for clarity.

(a)

(b)
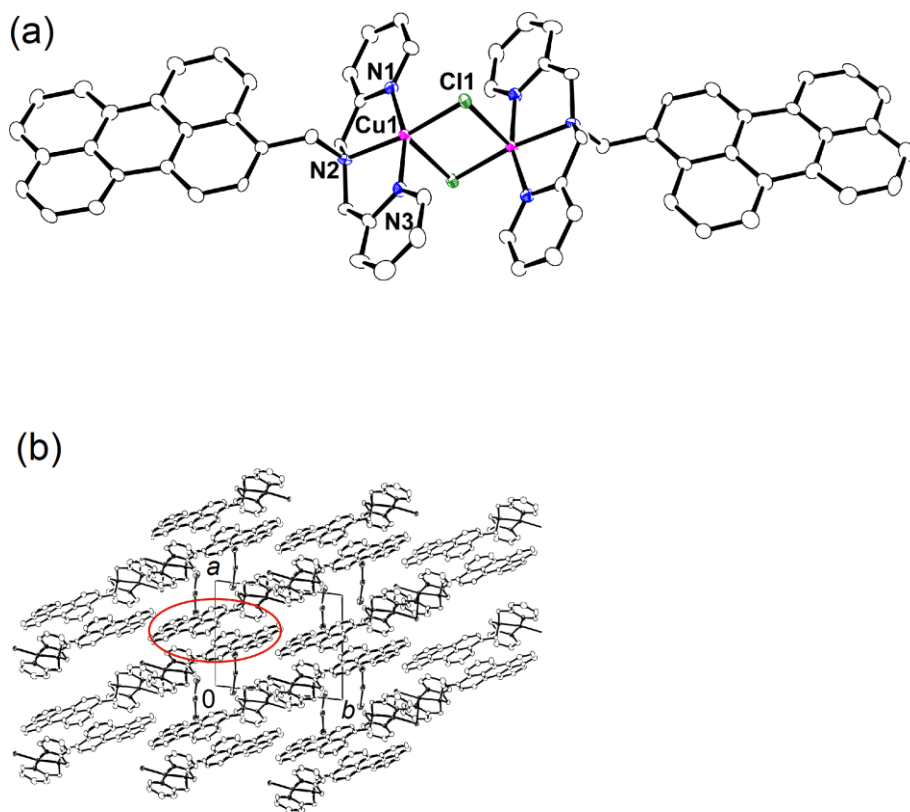
Figure 3. (a) Molecular structure of **3** in **3**·(I$_3$)$_2$ with thermal ellipsoids at 50% probability. (b) Packing view (*a*-axis projection) of **3**·(I$_3$)$_2$. A red ellipsoid represents a dimer of perylene moieties. Hydrogen atoms are omitted for clarity.
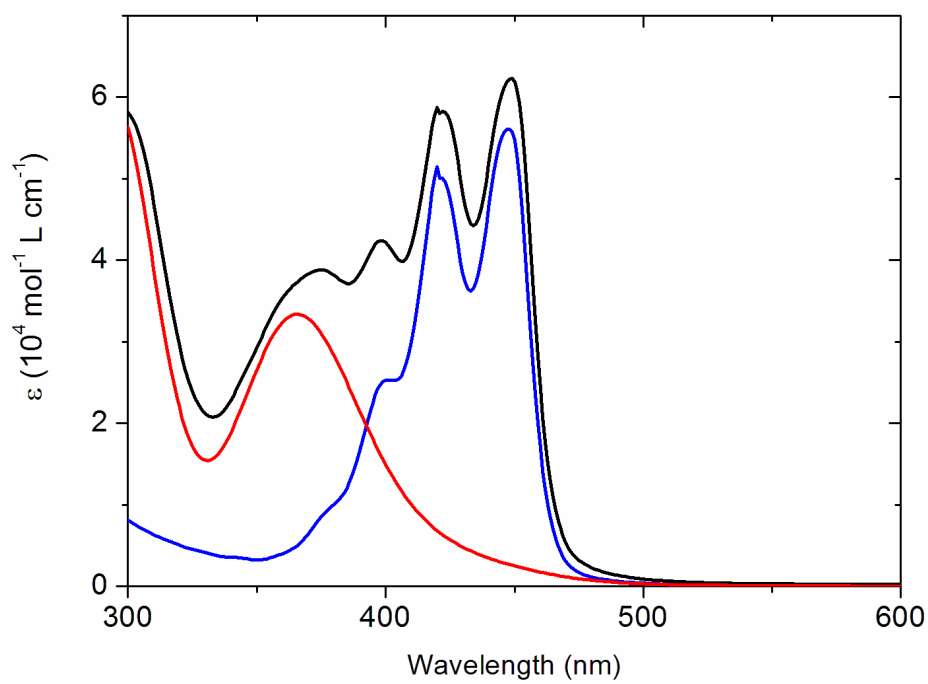
Figure 4. UV-vis absorption spectra for **2**·0.5H$_2$O (blue), **3**·I$_{5.6}$ (black), and *n*-Bu$_4$NI$_3$ (red) in DMF solution.
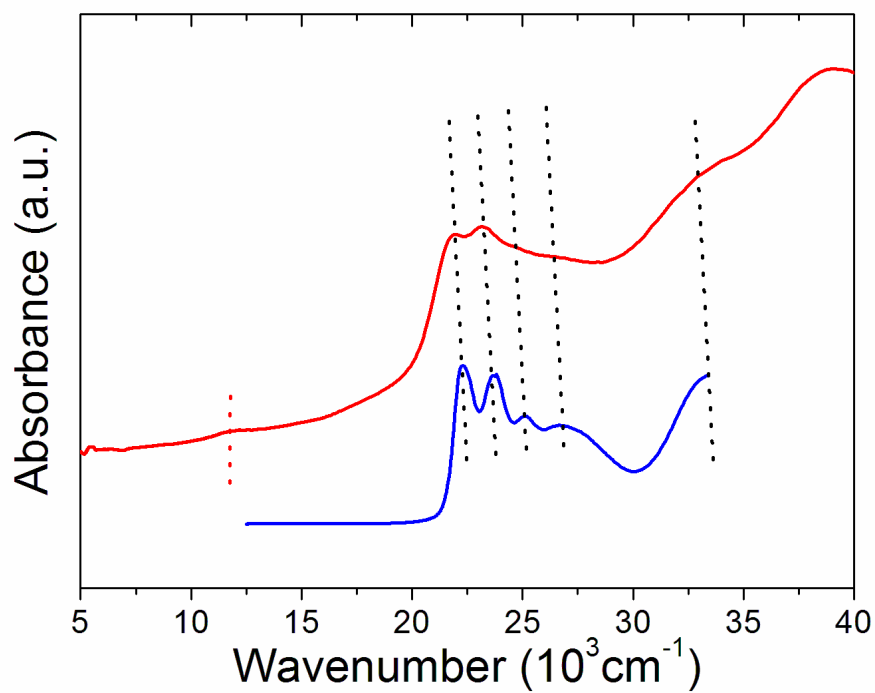
Figure 5. UV-vis absorption spectra for **3·I₅.₆** in DMF solution (blue), and in KBr pellet(red). Black dotted lines represent absorption peaks of perbpa moieties (see text). A red dotted line indicates the d-d transition of Cu(II).
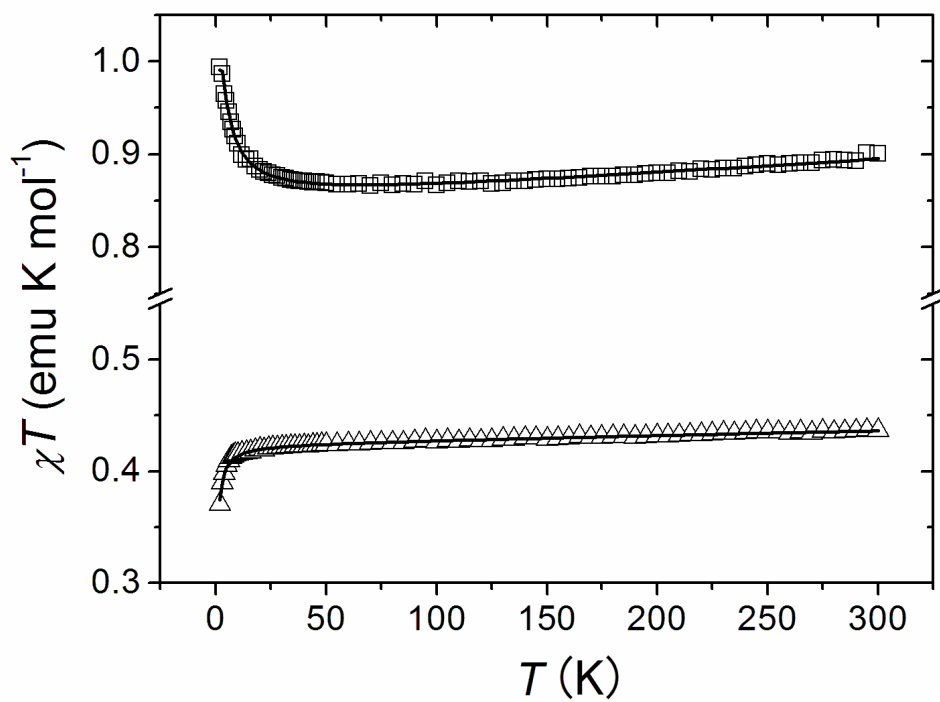
Figure 6. Temperature dependence of static susceptibilities for **2**·0.5H$_2$O (triangle) and **3**·I$_{5.6}$ (square). Solid lines over the data are the results of the curve fitting calculations (see text).
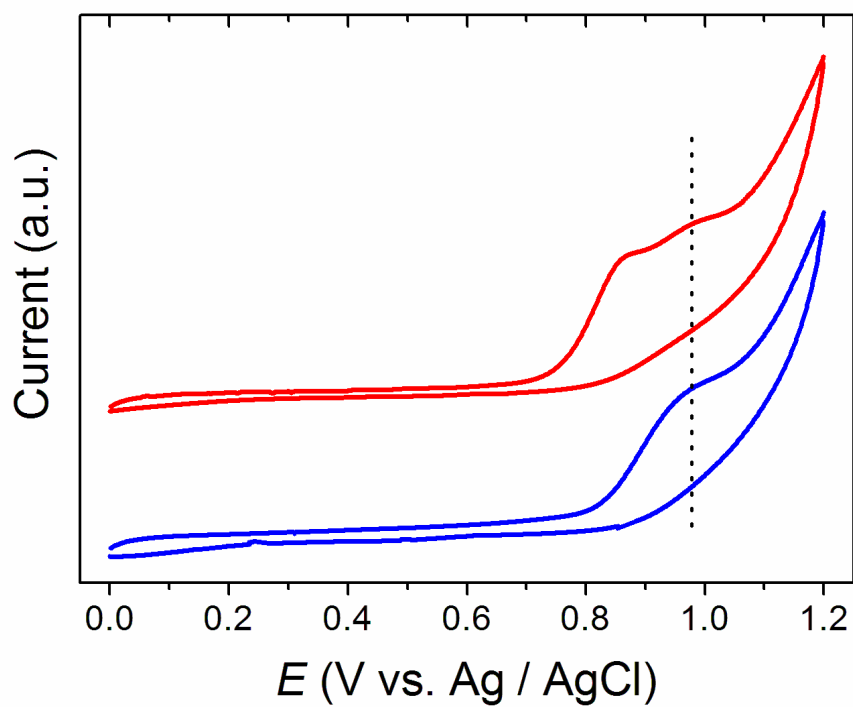
Figure 7. Cyclic voltammograms of **1** (red) and **2**·0.5H$_2$O (blue) in DMF solution. A dotted line represents the oxidation potential of perylene moieties (see text).

Table 1. Crystallographic data for perbpa and its copper complexes.

Compound	perbpa	[Cu(perbpa)Cl$_2$]·MeOH	[Cu$_2$(μ-Cl)$_2$(perbpa)$_2$](I$_3$)$_2$
	1	**2**·MeOH	**3**·(I$_3$)$_2$
Formula	C$_{33}$H$_{25}$N$_3$	C$_{34}$H$_{29}$Cl$_2$CuN$_3$O	C$_{66}$H$_{50}$Cl$_2$Cu$_2$I$_6$N$_6$
Formula weight	463.56	630.07	1886.58
Temperature (K)	293	133	133
Radiation (Å)	0.71073	0.71073	0.71073
Crystal system	orthorhombic	monoclinic	triclinic
a (Å)	10.418 (1)	8.113(5)	9.838(3)
b (Å)	11.722 (1)	25.62(1)	12.685(4)
c (Å)	38.869 (4)	13.660(8)	13.191(5)
a (°)			111.10(3)
β (°)		93.40(4)	99.08(3)
γ (°)			92.80(3)
V (Å^3)	4746.7 (7)	2834(2)	1506.6(9)
Space group	*Pbnb*	*P*2$_1$ / *n*	*P*$\bar{1}$
Z	8	4	1
D_{calcd} (g cm^{-3})	1.297	1.476	2.079
μ (mm^{-1})	0.076	0.993	3.918
Observed reflections	27820	48934	29122
Independent reflections	3560	6441	6839
Number of parameters	325	399	395
R_1 ($I > 2\sigma(I)$)	0.0767	0.07	0.064
wR_2 (all data)	0.2134	0.134	0.194
Goodness of fit	1.014	1.01	1.284

Table 2. Selected bond distances and angles for **2**·MeOH and **3**·(I$_3$)$_2$.

Bond Distances (Å)	**2**·MeOH	Bond Angles (°)	**2**·MeOH		
Cu1–N1	2.007 (4)	N1–Cu1–N2	80.7 (1)	N2–Cu1–Cl1	163.2 (1)
Cu1–N2	2.046 (4)	N1–Cu1–N3	160.8 (2)	N2–Cu1–Cl2	94.7 (1)
Cu1–N3	2.012 (4)	N1–Cu1–Cl1	96.8 (1)	N3–Cu1–Cl1	98.0 (1)
Cu1–Cl1	2.247 (1)	N1–Cu1–Cl2	92.3 (1)	N3–Cu1–Cl2	96.7 (1)
Cu1–Cl2	2.592 (1)	N2–Cu1–N3	81.7 (2)	Cl1–Cu1–Cl2	102.02 (4)
	3·(I$_3$)$_2$		**3**·(I$_3$)$_2$		
Cu1–N1	2.008 (6)	N1–Cu1–N2	81.8 (2)	N2–Cu1–Cl1	168.5 (1)
Cu1–N2	2.038 (4)	N1–Cu1–N3	163.0 (2)	N2–Cu1–Cl1'	95.7 (1)
Cu1–N3	1.992 (6)	N1–Cu1–Cl1	97.9 (1)	N3–Cu1–Cl1	97.3 (1)
Cu1–Cl1	2.257 (1)	N1–Cu1–Cl1'	93.7 (1)	N3–Cu1–Cl1'	92.2 (1)
Cu1–Cl1'	2.643 (1)	N2–Cu1–N3	81.8 (2)	Cl1–Cu1–Cl1'	95.71 (4)

Table 3. Oxidation peaks of DPV for **1** and **2**·0.5H$_2$O

E_{ox} (V *vs.* Ag/ AgCl)			
1	0.867	0.936	
2·0.5H$_2$O		0.942	
perylene		0.985	1.093

Table S1. Averaged bond lengths (*a-g*) of perylene group (Å) and intraplanar distances (*δ*) of perylene groups (Å)

	a	*b*	*c*	*d*	*e*	*f*	*g*
1	1.427 (4)	1.416 (5)	1.359 (5)	1.397 (5)	1.378 (4)	1.433 (4)	1.471 (4)
2·MeOH	1.414 (8)	1.391 (8)	1.396 (9)	1.389 (8)	1.401 (8)	1.410 (8)	1.476 (7)
3·$(I_3)_2$	1.448 (7)	1.41 (1)	1.38 (1)	1.407 (8)	1.38 (1)	1.43 (1)	1.485 (7)
perylene[ref.13]	1.424 (6)	1.400 (8)	1.370 (9)	1.418 (8)	1.397 (7)	1.425 (6)	1.471 (5)

	δ
1	3.45
2·MeOH	3.42
3·$(I_3)_2$	3.47
perylene	3.45

Table S2. Elemental analysis for **3**

	C(%)	H(%)	N(%)
found	43.13	2.52	4.34
calcd for $[Cu_2Cl_2(perbpa)]_2I_{5.6}$	43.18	2.75	4.58
calcd for $[Cu_2Cl_2(perbpa)]_2I_6$	42.02	2.67	4.45
calcd for $[Cu_2Cl_2(perbpa)]_2I_5$	45.05	2.86	4.78

Table S3. Oxidation peaks E_{ox} for **1**, **2**·0.5H_2O, and perylene in DMF (DPV).
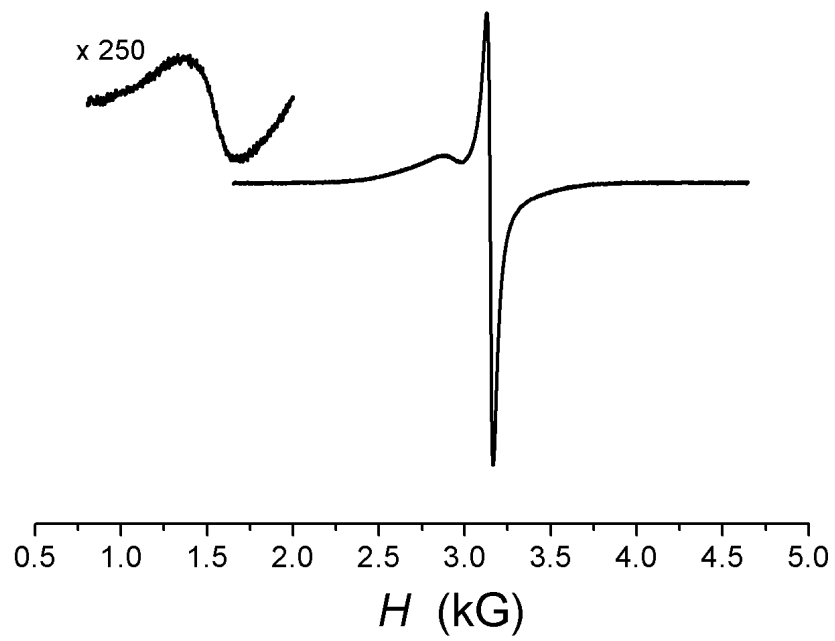
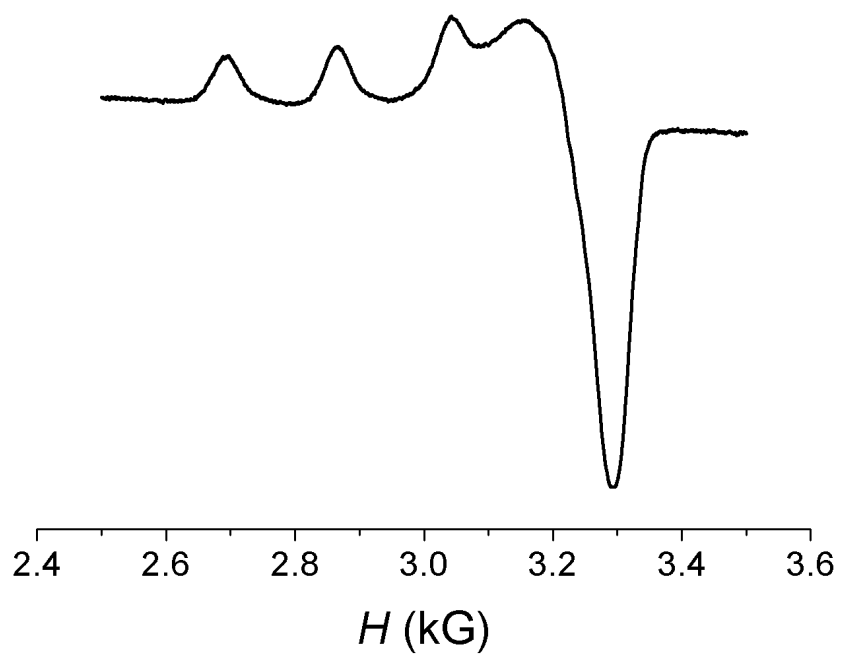| E_{ox} (V *vs.* Ag/ AgCl)		
1	0.867	0.936
2·0.5H_2O		0.942
perylene		0.985	1.093
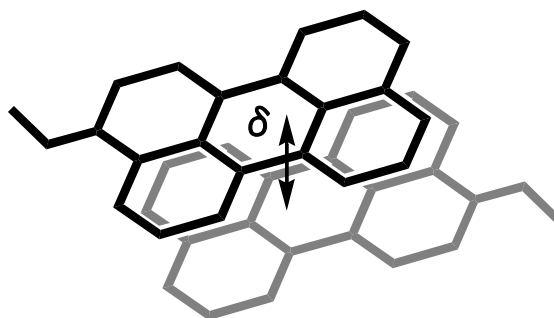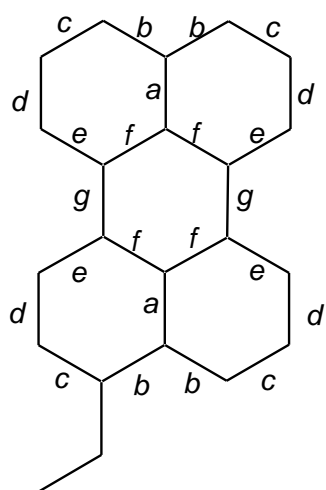
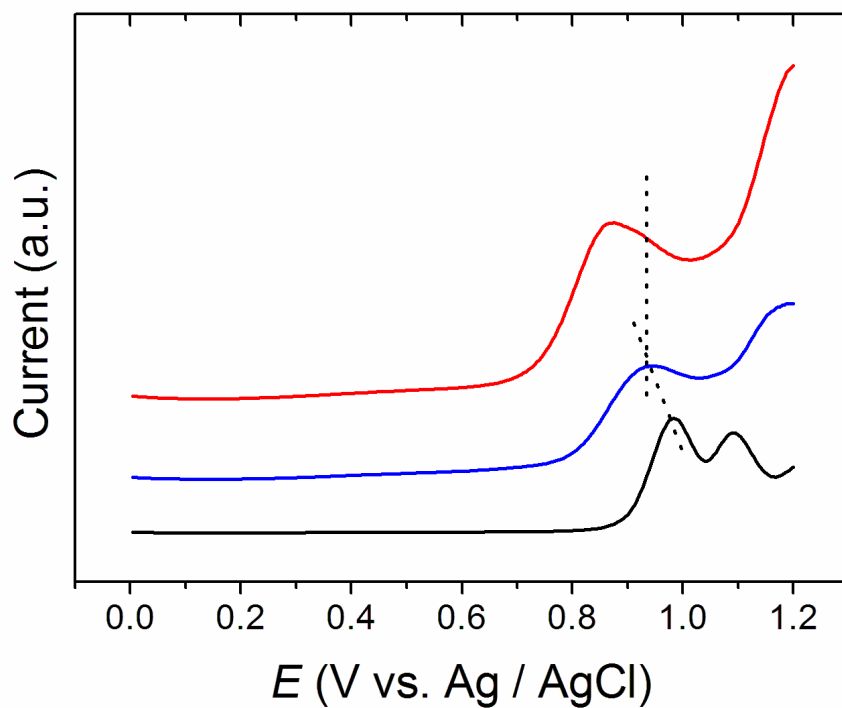**Figure S1**. Captions for Table S1
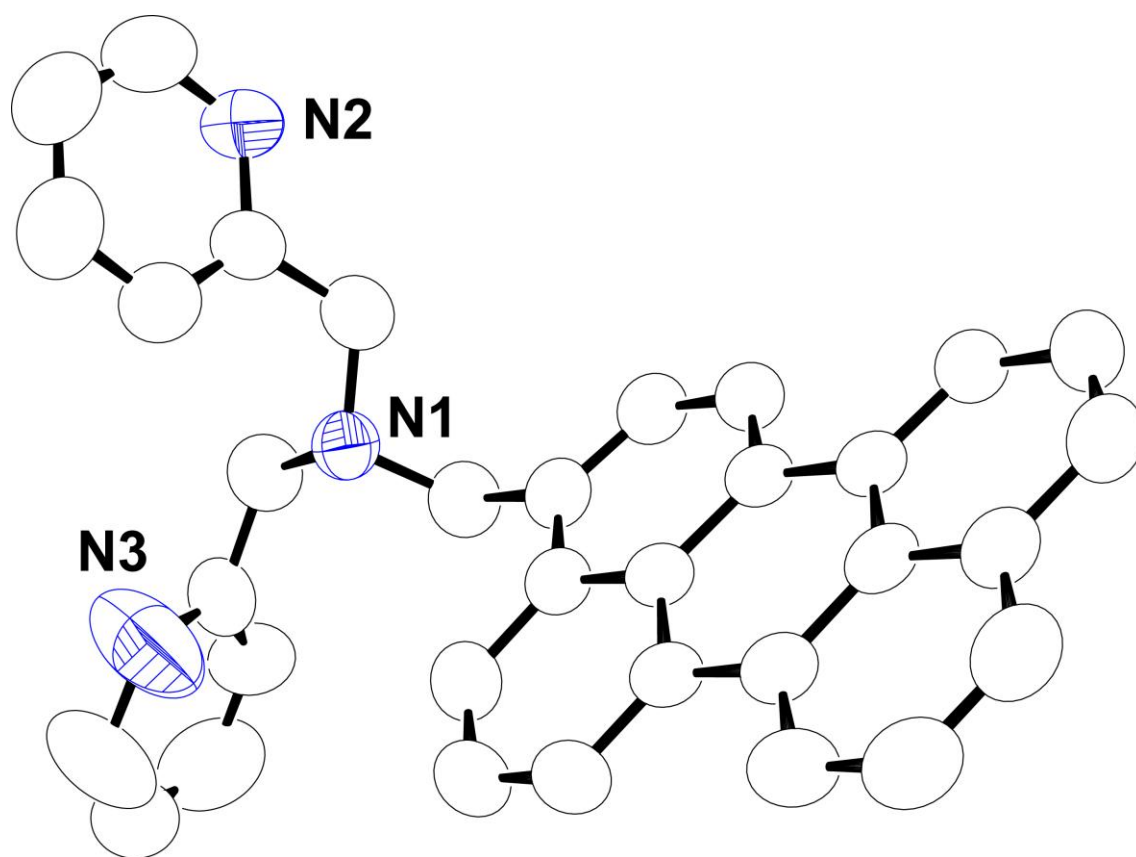
Figure S2. ORTEP view of perbpa (**1**) with thermal ellipsoids at 50 % probability. Hydrogen atoms are omitted for clarity.

x 250

H (kG)

Figure S3. X-band EPR spectra (powder) for **2**·0.5H$_2$O and **3**·I$_{5.6}$ at 4K.

Figure S4. X-band EPR spectrum (frozen DMF solution) for **3·I$_{5.6}$** at 77K.

Figure S5. Differential pulse voltammograms for **1** (red), **2** (blue), and perylene (black). Dotted lines represent the oxidation peak of perylene group (see text).